Analyst

Accepted Manuscript

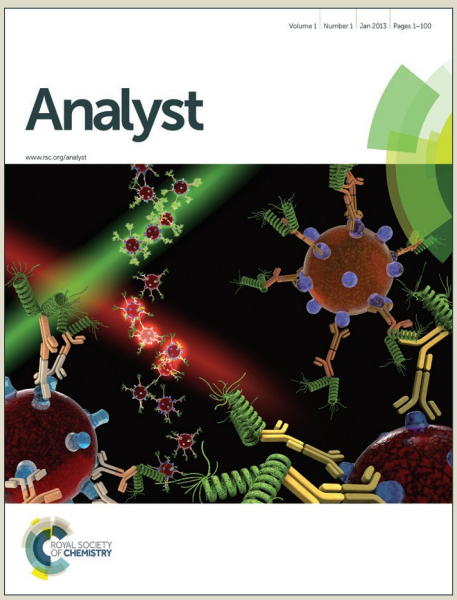

ROYAL SOCIETY OF CHEMISTRY

www.rsc.org/analyst

Journal Name

COMMUNICATION

Fluorescence array-based sensing of nitroaromatics using conjugated polyelectrolytes†

Received 00th January 20xx,
Accepted 00th January 20xx

DOI: 10.1039/x0xx00000x

www.rsc.org/

Jiatao Wu,[a,b] Chunyan Tan,*[a,b] Zhifang Chen,[a,b] Yu Zong Chen,[c] Ying Tan,*[a,b] and Yuyang Jiang[b,d]

A sensor array consisting of six cationic fluorescent conjugated polyelectrolytes (CPEs) is reported, which could readily differentiate nine closely related hydrophilic nitroaromatics (NACs) in separate aqueous solutions by fluorescence pattern recognition and linear discrimination analysis (LDA).

Fast and reliable detection of hazardous nitroaromatics (NACs) is crucial for homeland security, environmental monitoring, coal explorations, and military operations.[1-3] NACs, such as picric acid and 2,4,6-trinitrotoluene, are widely used in manufacturing of explosives and blasting in engineering, leading to environmental contaminations.[4, 5] In addition, hydrophilic NAC pollutants in water sources are related to several diseases, including gastritis, hepatitis, anaemia, cataract, and severe neurological damage.[6-8] Therefore, suitable sensors with high sensitivity and selectivity for identification of trace NACs in water bodies are in urgent demand for environmental protection and sustainable development.

Currently, a wide range of instrumental techniques, such as mass spectrometry (MS), X-ray diffraction (XRD), nuclear quadrupole resonance (NQR), and cyclic voltammetry (CV), are available for NACs detection.[9, 10] Although these methods provide advantages, their use is limited due to strong reliability on expensive instruments, complicated operations, and inability to transport. Optical sensors provide alternative methods for NACs detection, as they exhibit high sensitivity, selectivity, portability, and cost-effectiveness.[11-14] Among fluorescent materials, conjugated polymers (CPs) have attracted significant research attention and have been applied in chemo- and bio-sensing due to their strong light absorption and fluorescence emission, as well as high sensitivity to small perturbations.[15-18] For example, Swager *et al.* utilized fluorescent porous CP films for detection of explosive vapors containing TNT.[19] In addition to specific biosensing, where one CP is used to target one analyte, CPs are also applied to the construction of array-based sensors to screen series of structures or property-similar analytes, such as proteins, metal ions, and cancerous cells.[20-22]

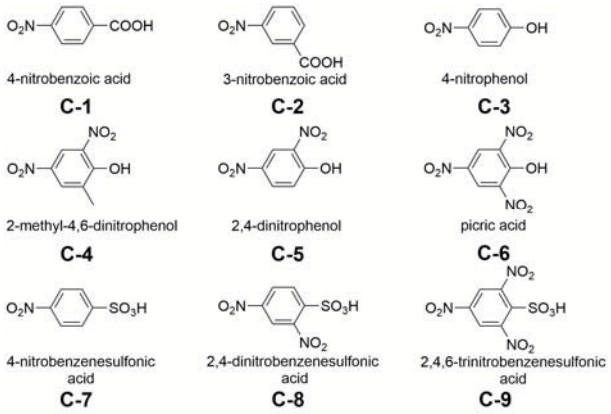

Scheme 1. Structures of the nine nitroaromatics (NACs)

Herein, we report an effective fluorescence array-based sensing method of NACs using six conjugated polyelectrolytes (six-CPEs) with the ability to differentiate nine NACs. These nine NACs include 4-nitrobenzoic acid (C-1), 3-nitrobenzoic acid (C-2), 4-nitrophenol (C-3), 2-methyl-4,6-dinitrophenol (C-4), 2,4-dinitrophenol (C-5), picric acid (C-6), 4-nitrobenzenesulfonic acid (C-7), 2,4-dinitrobenzenesulfonic acid (C-8), 2,4,6-trinitrobenzensulfonic acid (C-9). The respective structures are illustrated in Scheme 1.

CPEs with cationic groups have attracted much interest because of their potential application in detecting different analytes, such as DNA, proteins, hydrogen peroxide, hydrogen and peroxide.[23-30] In this study, six CPEs were synthesized by Pd-catalysed Sonogashira coupling (structures are shown in Scheme 2). Among the six CPEs, P1, P2, and P3 shared the

[a] Department of Chemistry, Tsinghua University, Beijing 100084, P. R. China
[b] The Ministry-Province Jointly Constructed Base for State Key Lab- Shenzhen Key Laboratory of Chemical Biology, The Graduate School at Shenzhen, Tsinghua University, Shenzhen 518055, P. R. China. E-mail: tancy@sz.tsinghua.edu.cn; tan.ying@sz.tsinghua.edu.cn
[c] Shenzhen Kivita Innovative Drug Discovery Institute, Shenzhen 518055, China
[d] Department of Pharmacology and Pharmaceutical Sciences, School of Medicine, Tsinghua University, Beijing 100084, P. R. China.

† Electronic Supplementary Information (ESI) available: [details of any supplementary information available should be included here]. See DOI: 10.1039/x0xx00000x

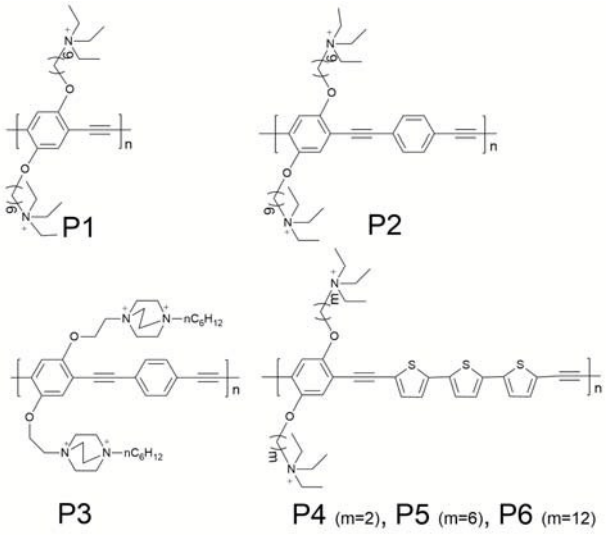

Scheme 2. Structures of six cationic conjugated polyelectrolytes (CPEs)

same poly(*p*-pheynylene ethynylene) backbones, whereas P4,P5 and P6 have a backbone of poly(p-phenylene ethynylene terthiophene), and have the same quaternary ammonium salt as terminal hydrophilic groups with different aliphatic chain lengths.[31] The molecular weight of the six CPEs were determined using matrix-assisted laser desorption ionization (MALDI) mass spectrometry and are listed in Table 1. Generally, the $\overline{M_n}$ and $\overline{M_w}$ values ranged between 11.7 and 16.8 kDa, 18.4 and 25.8 kDa, respectively, giving polydispersity indices (PDI) between 1.50 and 1.65, which is reasonable for step-growth polycondensation.

Previous reports suggested that polymers P4-P6 demonstrated similar photophysical properties as P1-P3.[29-32] However, due to different backbone structures, conjugation lengths, aggregation states, and side groups, the absorption and fluorescence spectra display some differences. For example, the introduction of terthiophene units into the backbone lowered the band gap of P4-P6 compared to P1-P3, resulting in a 15-50 nm red-shifted absorption band, as shown in Fig. 1a. The shorter side chains of P4 made it less aggregated in aqueous solution, demonstrating a greater quantum yield than P5 and P6 with a more structured emission band at a shorter wavelength (Fig. 1b).

It has been reported that NACs can efficiently quench the fluorescence of CPEs by means of electron transfer from the

Table 1 Characterization data of P1-P6.

Polymer	$\overline{M_n}$ $(\times 10^3\ Da)^a$	$\overline{M_w}$ $(\times 10^3\ Da)^a$	PDI^b	$\overline{x_n}$	λ_{max}^{abs} (nm)	λ_{max}^{em} (nm)
P1	12.2	18.4	1.51	35	386	470
P2	15.0	22.6	1.50	26	429	462
P3	11.7	19.2	1.65	18	400	490
P4	16.8	25.8	1.53	26	461	457
P5	13.3	20.4	1.53	19	479	554
P6	14.6	23.4	1.60	19	444	560

[a]Molecular weights were measured on a 4700 Proteomics Analyzer MALDI-TOF/TOF-MS using 2,5-dihydroxybenzoic acid (DHB) as the matrix.
[b]Obtained according to formula PDI=$\overline{M_n}/\overline{M_w}$

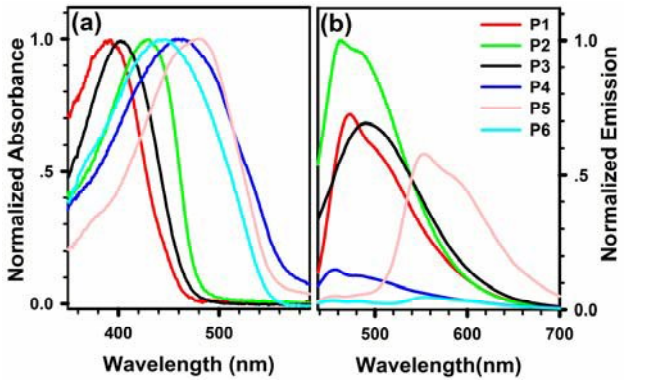

Fig. 1 UV–visible absorption (a) and fluorescence emission spectra (b) of P1 (red), P2 (green), P3 (black), P4 (blue), P5 (pink) and P6 (cyan) in aqueous solution (λ_{ex}=415). Emission spectra were normalized to reflect relative quantum yields.

excited polymers to the electron acceptor in NACs.[33] However, selectivity is difficult to achieve using a single CPE. In 2008, Knapp *et al* discriminated NACs and explosives mimics by a fluorescent Zn(salicylaldimine) sensor array.[34] Therefore, instead of just a single response of a given polymer to one specific analyte, CPE-based sensor arrays can facilitate analysis of a combination of responses.[20-22] In this study, quenching analysis of the 6 polymers by 9 NACs was carried out in order to build response patterns. The responses were calculated as the ratio of fluorescence intensity at emission, I_0/I, where I_0 and I were the fluorescence intensities of each CPE without and with NACs, respectively. Fingerprint analyses were carried out using 9 NACs, all with the concentration of 1.0 μM. As shown in Fig. 2, the bar graph demonstrates different quenching responses. We speculated that the interaction between the polymer and NACs as well as the redox potentials of the NACs played very important roles in determining the quenching efficiency. For example, P3 has more positive charges on each polymer repeat unit compared to P1 and P2, and thus shows stronger fluorescence quenching when the NAC analyte is negatively charged due to stronger electrostatic attraction. For P4, P5 and P6, which shared the same backbone structure, the binding affinities are different due to polymer's different lengths of ionic side chains. Specifically speaking, P4 with the shortest side chains showed the lowest quenching

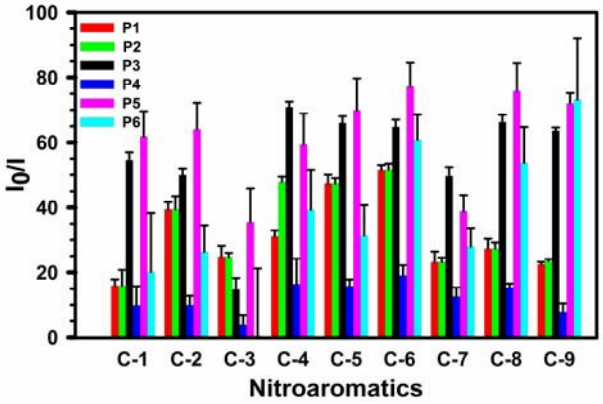

Fig. 2 Response patterns constructed based on fluorescence quenching of the six CPEs by nine NACs at 1 μM each.

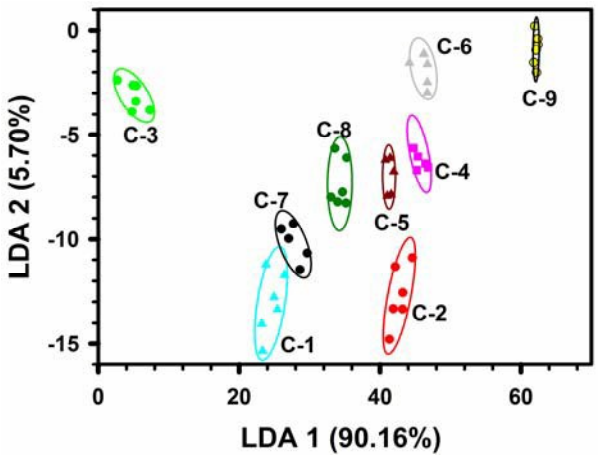

Fig. 3 2-D canonical score plot of the fluorescence response patterns obtained by six-CPE sensor array against nine NACs at 1.0 μM concentration.

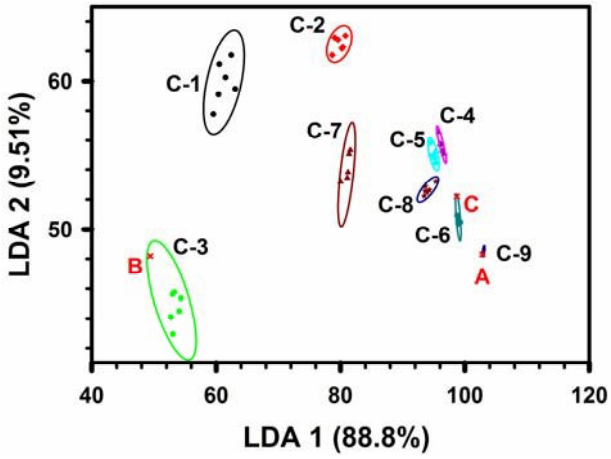

Fig. 5 2-D canonical score plot of the fluorescence response patterns obtained by six-CPE sensor array (A_{420} = 0.1) against three unknown samples (A_{300} = 0.05).

efficiency to any NAC analyte compared to P5 and P6. Furthermore, compared to C-2 without charges, the CPEs were quenched more efficiently by NACs with charged C-1, C-2, and C-7. Furthermore, trinitro-substituted NACs showed higher quenching abilities than both dinitro-substituted and mononitro-substituted NACs.

In this analysis, fluorescence data were collected in six replicates and subjected to LDA using R software (i3863.0.3). It was transformed into four canonical scores (90.16%, 5.7%, 2.3%, and 0.9% variation). The first two factors accounted for 95.86% of the variance and were used to construct the two-dimensional discrimination plot. As shown in Fig. 3, the horizontal and vertical axes have 90.16% and 5.7% weighting, respectively. Each dot represents the fluorescence response of the six-CPE sensor array to a single NAC concentration. The results for the nine different NACs are clearly clustered into nine non-overlapping eclipses. Mononitro-substituted NACs (C-1, C-2, C-3, C-7) were separated from dinitro-substituted NACs (C-4, C-5, C-8). Picric acid (C-6) and 2,4,6-trinitrobenzenesulfonic acid (C-9) were well separated from the others due to their high quenching efficiency.

Further classification experiments were tested in which the absorbance of NACs, A_{300}, was fixed at 0.05 at 300 nm, at which the concentration of NACs was in the range of 7 to 100 μ M approximately, depending on the different molar extinction coefficients. The resulting data were analyzed and transformed into four scores through LDA using R software, which accounted for 94.74%, 3.78%, 1.19%, and 0.2% variation. The first two factors were used to construct the two-dimensional discrimination plot, as shown in Fig. 4. Each dot represented the fluorescence response of the six-CPE sensor array to a single NAC concentration. Obviously, the results for the nine different NACs are clustered into nine non-overlapping groups.

To explore the potential application of each array to NACs analysis, we tested the six-CPE sensor array to quantify unknown NACs in aqueous solution. Three samples were selected randomly from the nine NACs to avoid the influence of anthropogenic. The array response to each unknown sample (A_{300} = 0.05) was compared to classification data and unknown samples were identified according to their placement in this 2-D space in Fig. 5 with a 95% confidence interval. The three unknown samples were identified with 100% accuracy.

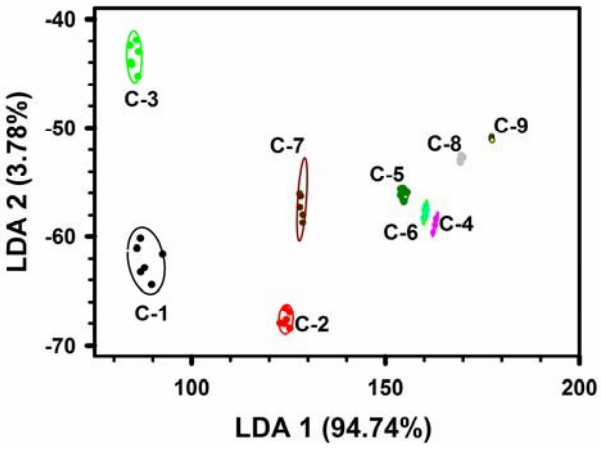

Fig. 4 2-D canonical score plot of the fluorescence response patterns obtained by six-CPE sensor array (A_{420} = 0.1) against nine NACs (A_{300} = 0.05).

Conclusions

In conclusion, a sensor array consisting of six cationic CPEs was designed for detecting nine NACs. The varying binding affinity gave rise to distinct fluorescence response via polymer-nitroaromatic interactions and fluorescence quenching. Nine NACs were differentiated successfully in aqueous solution both at a concentration of 1.0 μM and at a fixed absorbance of 0.05 at 300 nm by 2-D discriminant patterns. Furthermore, our six-CPE sensor array provided a practical and efficient method to determine the unknown samples with 100% accuracy.

Acknowledgements

This work is supported by grants from Natural Science Foundation of China (No. 21572115 and 21302108), Shenzhen Municipal Government (CXB201104210014A and

20150113A0410006), and Shenzhen Reform Commission (Disciplinary Development Program for Chemical Biology).

Notes and references

1 S. Letzel, T. Goen, M. Bader, J. Angerer and T. Kraus, *Occup. Environ. Med.*, 2003, **60**, 483-488.
2 B. M. Luccioni, R. D. Ambrosini and R. F. Danesi, *Proc. Inst. Civ. Eng. Struct. Build.*, 2005, **158**, 1-12.
3 D. R. S. Lima, M. L. S. Bezerra, E. B. Neves and F. R. Moreira, *Rev. Environ. Health*, 2011, **26**, 101-110.
4 J. Neuwoehner, A. Schofer, B. Erlenkaemper, K. Steinbach, K. Hund-Rinke and A. Eisentraeger, *Environ. Toxicol. Chem.*, 2007, **26**, 1090-1099.
5 K.-S. Ju and R. E. Parales, *Microbiol. Mol. Biol. Rev.*, 2010, **74**, 250-+.
6 B. M. Hasspieler, G. D. Haffner and K. Adeli, *J. Toxicol. Environ. Health*, 1997, **52**, 137-148.
7 V. Purohit and A. K. Basu, *Chem. Res. Toxicol.*, 2000, **13**, 673-692.
8 T. Grummt, H. G. Wunderlich, A. Chakraborty, M. Kundi, B. Majer, F. Ferk, A. K. Nersesyan, W. Parzefall and S. Knasmuller, *Environ. Mol. Mutagen.*, 2006, **47**, 95-106.
9 D. S. Moore, *Rev. Sci. Instrum.*, 2004, **75**, 2499-2512.
10 J. S. Caygill, F. Davis and S. P. J. Higson, *Talanta*, 2012, **88**, 14-29.
11 M. S. Meaney and V. L. McGuffin, *Anal. Bioanal. Chem.*, 2008, **391**, 2557-2576.
12 Y. Salinas, R. Martinez-Manez, M. D. Marcos, F. Sancenon, A. M. Costero, M. Parra and S. Gil, *Chem. Soc. Rev.*, 2012, **41**, 1261-1296.
13 Z. Hu, B. J. Deibert and J. Li, *Chem. Soc. Rev.*, 2014, **43**, 5815-5840.
14 D. Banerjee, Z. Hu and J. Li, *Dalton Trans.*, 2014, **43**, 10668-10685.
15 D. T. McQuade, A. E. Pullen and T. M. Swager, *Chem. Rev.*, 2000, **100**, 2537-2574.
16 S. W. Thomas, G. D. Joly and T. M. Swager, *Chem. Rev.*, 2007, **107**, 1339-1386.
17 H. Jiang, P. Taranekar, J. R. Reynolds and K. S. Schanze, *Angew. Chem. Int. Ed.*, 2009, **48**, 4300-4316.
18 C. Zhu, L. Liu, Q. Yang, F. Lv and S. Wang, *Chem. Rev.*, 2012, **112**, 4687-4735.
19 J.-S. Yang and T. M. Swager, *J. Am. Chem. Soc.*, 1998, **120**, 11864-11873.
20 O. R. Miranda, C.-C. You, R. Phillips, I.-B. Kim, P. S. Ghosh, U. H. F. Bunz and V. M. Rotello, *J. Am. Chem. Soc.*, 2007, **129**, 9856-+.
21 A. Bajaj, O. R. Miranda, R. Phillips, I.-B. Kim, D. J. Jerry, U. H. F. Bunz and V. M. Rotello, *J. Am. Chem. Soc.*, 2010, **132**, 1018-1022.
22 Y. Wu, Y. Tan, J. Wu, S. Chen, Y. Z. Chen, X. Zhou, Y. Jiang and C. Tan, *ACS Appl. Mater. Interfaces*, 2015, **7**, 6882-6888.
23 F. He, Y. L. Tang, S. Wang, Y. L. Li and D. B. Zhu, *J. Am. Chem. Soc.*, 2005, **127**, 12343-12346.
24 F. He, Y. L. Tang, M. H. Yu, S. Wang, Y. L. Li and D. B. Zhu, *Adv. Funct. Mater.*, 2006, **16**, 91-94.
25 X. Duan, Z. Li, F. He and S. Wang, *J. Am. Chem. Soc.*, 2007, **129**, 4154-+.
26 F. Feng, Y. Tang, F. He, M. Yu, X. Duan, S. Wang, Y. Li and D. Zhu, *Adv. Mater.*, 2007, **19**, 3490-+.
27 K.-Y. Pu and B. Liu, *Macromolecules*, 2008, **41**, 6636-6640.
28 X. Duan, L. Liu, F. Feng and S. Wang, *Acc. Chem. Res.*, 2010, **43**, 260-270.
29 Y. Xie, R. Zhao, Y. Tan, X. Zhang, F. Liu, Y. Jiang and C. Tan, *ACS Appl. Mater. Interfaces*, 2012, **4**, 405-410.
30 Y. Xie, Y. Tan, R. Liu, R. Zhao, C. Tan and Y. Jiang, *ACS Appl. Mater. Interfaces*, 2012, **4**, 3784-3787.
31 Z. Chen, P. Wu, R. Cong, N. Xu, Y. Tan, C. Tan and Y. Jiang, *ACS Appl. Mater. Interfaces*, 2016, **8**, 3567-3574.
32 Y. Tang, E. H. Hill, Z. Zhou, D. G. Evans, K. S. Schanze and D. G. Whitten, *Langmuir*, 2011, **27**, 4945-4955.
33 D. Zhao and T. M. Swager, *Macromolecules*, 2005, **38**, 9377-9384.
34 M. E. Germain and M. J. Knapp, *J. Am. Chem. Soc.*, 2008, **130**, 5422-5423.